

## Enhanced crystallinity and optical properties of GaN pyramids structures with $\text{Al}_{1-x}\text{Ga}_x\text{N}/\text{GaN}$ superlattices by SAG technique

B. K. Kang<sup>a</sup>, M. O. Kim<sup>a</sup>, K. M. Song<sup>b</sup> and D. H. Yoon<sup>a,\*</sup>

<sup>a</sup>School of Advanced Materials Science & Engineering, Sungkyunkwan University, Suwon, 440-746, Republic of Korea

<sup>b</sup>Korea Advanced Nano Fab Center (KANC), Iui-dong, Suwon, 906-10, Republic of Korea

This study examined the effects of (5, 10) pair of  $\text{Al}_{1-x}\text{Ga}_x\text{N}/\text{GaN}$  superlattices based (25, 50 nm) HT-AlN on the optical properties and crystallinity of GaN pyramids and InGaN/GaN multiple quantum wells. High resolution X-ray diffraction revealed 10-pair of  $\text{Al}_{1-x}\text{Ga}_x\text{N}/\text{GaN}$  superlattices on a 50 nm HT-AlN buffer layer to have the narrowest full width at half maximum of  $1.215^\circ$  because the  $\text{Al}_{1-x}\text{Ga}_x\text{N}/\text{GaN}$  superlattices prevent the dislocations generated at the interface between the AlN buffer layer and Si substrates from propagating to the surface of GaN. The optical properties and emission region of InGaN/GaN multiple quantum wells on the GaN pyramids were observed by photoluminescence and cathodoluminescence measurements.

**Key words:** High resolution X-ray diffraction, Superlattices, Selective epitaxy, Nitride, Semiconducting III-V materials.

### Introduction

III-nitride based semiconductors have been used extensively for a decade due to the possibility of high power, high temperature devices and optical devices. The growth of GaN on Si substrates has been pursued due to the low substrate cost and good conductivity compared to sapphire and SiC. However, epitaxial GaN films on Si substrates have cracks and a high dislocation density of approximately  $10^8 \sim 10^{10} \text{ cm}^{-2}$  on the surface due to tensile stress induced by the large lattice mismatch (-16.9%) and different thermal expansion coefficient (54%) between the GaN film and Si substrate [1-4]. To reduce the high dislocation density of GaN films on Si, GaN films were grown on a variety of buffer layers, such as ZnO, GaN and AlN [5-7]. AlN was reported to be a desirable buffer layer for GaN epitaxy on Si substrates. The compressive stress induced in the grown AlN buffer layer can compensate for the tensile stress in GaN grown on Si. Unfortunately, the thin AlN buffer layer exhibited a tensile stress that caused cracking problems in the GaN films on Si substrates while cooling from the growth temperature of GaN to room temperature. In addition, the GaN film on Si substrates had a high dislocation density [8-10].

Recently, one of the methods to overcome these problems is to insert GaN/ $\text{Al}_x\text{Ga}_{1-x}\text{N}$  superlattices (SLs) and a graded AlGa<sub>x</sub>N between the GaN structures and buffer layers. The

GaN/ $\text{Al}_x\text{Ga}_{1-x}\text{N}$  SLs not only compensates for the tensile stress because the GaN/ $\text{Al}_x\text{Ga}_{1-x}\text{N}$  SLs inter layer induce compressive stress with negative lattice mismatch between GaN and AlN at low Al mole fractions, but also prevents the dislocations from propagating and generating in GaN epitaxial films [11-12].

The GaN pyramids fabricated using a selective area growth (SAG) technique have been reported to offer many advantages, such as the easy control of facets and shapes, absence and contamination of any physical damage by dry etching, increased radiation surface and avoidance of propagating and bend threading dislocations in the three dimensional structures [13-15].

This paper reports the effects of the high temperature (HT)-AlN buffer layer thickness and pair of  $\text{Al}_{1-x}\text{Ga}_x\text{N}/\text{GaN}$  SLs on GaN pyramid and InGaN/GaN multiple quantum wells (MQWs) grown using the SAG technique. The optical and crystal quality of the GaN pyramid and InGaN/GaN MQWs were examined to discuss the role of the  $\text{Al}_{1-x}\text{Ga}_x\text{N}/\text{GaN}$  SLs.

### Experimental procedures

All the samples were fabricated by metalorganic chemical vapor deposition. For the SAG technique, the  $\text{SiO}_2$  mask was deposited by plasma-enhanced chemical vapor deposition at 300 °C and 2- $\mu\text{m}$  dot patterns were formed on the Si (111) substrates. The dots patterned on the Si (111) substrates were cleaned thermally in  $\text{H}_2$  ambient at 1100 °C for 10 min. The patterned dot was prefilled with trimethyl-aluminum (TMAI) to prevent the formation of  $\text{SiN}_x$  on opened Si substrates. Two different thicknesses (25, 50 nm) of HT-AlN buffer layers and (5, 10 pair)  $\text{Al}_{1-x}\text{Ga}_x\text{N}/\text{GaN}$  SLs based HT-

\*Corresponding author:  
Tel : +82 31 290 7361  
Fax: +82 31 290 7371  
E-mail: dhyoon@skku.edu

AlN buffer layers were deposited at 1070 °C and 1140 °C, respectively. TMAI, Trimethyl-gallium (TMGa) and NH<sub>3</sub> were used as the Al, Ga and N precursors for the AlN buffer layer and Al<sub>1-x</sub>Ga<sub>x</sub>N/GaN SLs, respectively. The V/III of the HT-AlN buffer layer was 1584. The flow rate of TMGa, TMAI and NH<sub>3</sub> for growing the Al<sub>1-x</sub>Ga<sub>x</sub>N/GaN SLs was  $4.418 \times 10^{-4}$  mol/min,  $3.488 \times 10^{-5}$  mol/min and  $8.929 \times 10^{-2}$  mol/min, respectively. TMGa, triethyl-gallium (TEGa), trimethyl-indium (TMIn) and NH<sub>3</sub> were used as the Ga, N and In precursors, respectively, for the GaN pyramid structures and InGaN/GaN MQWs at growth temperatures of 1045 °C and 800 °C, respectively. The crystal quality of the GaN pyramid structures were investigated from the rocking curve of GaN (0002) by high resolution X-ray diffraction (HR-XRD). The morphological changes in the as-grown samples were examined by field-emission scanning electron microscopy (FE-SEM). Photoluminescence (PL) and cathodoluminescence (CL) measurements were used to investigate the optical properties of the GaN pyramids and 3-pair InGaN/GaN MQWs at room temperature.

## Results and discussion

HRXRD rocking curve were obtained to characterize the crystal quality of the GaN pyramid structures as function of the HT-AlN (25, 50 nm) and Al<sub>1-x</sub>Ga<sub>x</sub>N/GaN/GaN SLs based HT-AlN buffer layer using the SAG technique. The crystal quality of the GaN epi layer was estimated from the full width at half maximum (FWHM). Fig. 1 shows the (0002) rocking curve of the grown GaN pyramid structures at various HT-AlN (25, 50 nm) and Al<sub>1-x</sub>Ga<sub>x</sub>N/GaN SLs based HT-AlN buffer layers. The FWHM of the GaN pyramid structures with HT-AlN buffer layer increased from 2.625 ° to 1.685 ° when the thickness of the AlN layer was increased from 25 nm to 50 nm. The effects of the changed pair of Al<sub>1-x</sub>Ga<sub>x</sub>N/GaN SLs to improve the crystal quality of the GaN pyramid structures were examined. The intensity of the rocking curve increased

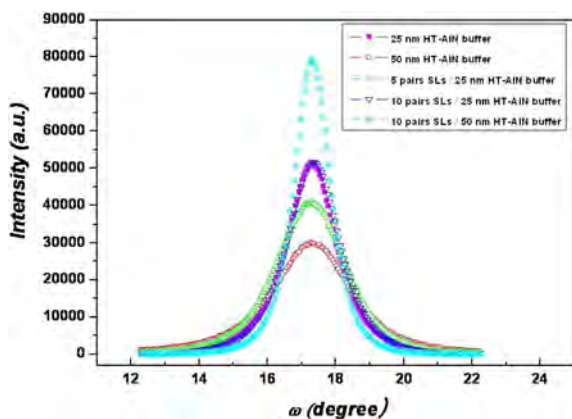


**Fig. 1.**  $\omega$  scans of symmetric reflection (0002) on the GaN pyramids at Al<sub>1-x</sub>Ga<sub>x</sub>N/GaN SLs based HT-AlN buffer layer.

and the FWHM decreased with increasing pair of Al<sub>1-x</sub>Ga<sub>x</sub>N/GaN SLs-based HT-AlN buffer layers. These results were attributed to the improved crystal quality of the GaN pyramid structures by Al<sub>1-x</sub>Ga<sub>x</sub>N/GaN SLs because the Al<sub>1-x</sub>Ga<sub>x</sub>N/GaN SLs prevent the dislocations generated at the interface AlN buffer layer and Si substrates from propagating to the surface of GaN and compensate induced stress between GaN and Si substrates [16]. However, in the case of the 5 and 10 pair Al<sub>1-x</sub>Ga<sub>x</sub>N/GaN SLs based 25 nm HT-AlN buffer layer, the Al<sub>1-x</sub>Ga<sub>x</sub>N/GaN SLs decreased the crystal quality. On the other hand, the crystal quality of the 10-pair Al<sub>1-x</sub>Ga<sub>x</sub>N/GaN SLs based 50 nm HT-AlN buffer layer was improved dramatically. The FWHM of the rocking curve at 10-pair of Al<sub>1-x</sub>Ga<sub>x</sub>N/GaN SLs on 50 nm HT-AlN was narrowest at 1.215 °. This may be due to a change in the composition of the Al<sub>1-x</sub>Ga<sub>x</sub>N/GaN SLs according to different depths from the AlN surface to the SiO<sub>2</sub> surface because the diffusion length of Ga atoms is longer than that of Al atoms in the vapor phase [17].

The surface morphology of the GaN pyramid and InGaN/GaN MQWs on the 10-pair of Al<sub>1-x</sub>Ga<sub>x</sub>N/GaN SLs based 50 nm HT-AlN buffer layer were examined by FESEM. The plane view and cross section image of the lateral grown 5- $\mu$ m GaN pyramid and InGaN/GaN MQWs by the SAG technique were observed, as shown Fig. 2. The GaN pyramid and InGaN/GaN MQWs were grown selectively on the synthesized HT-AlN buffer layer and Al<sub>1-x</sub>Ga<sub>x</sub>N/GaN SLs dot patterns

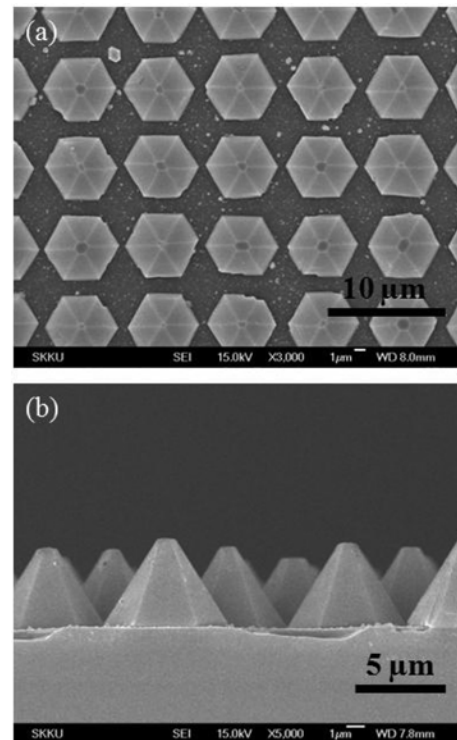


**Fig. 2.** The plan view (a) and cross section (b) FE-SEM images of the GaN pyramids and InGaN/GaN MQWs on the 10-pair Al<sub>1-x</sub>Ga<sub>x</sub>N/GaN SLs based 50 nm HT-AlN.

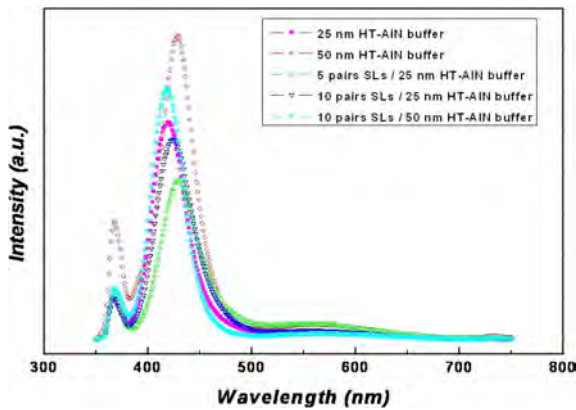


**Fig. 3.** PL spectrum of the GaN pyramids and InGaN/GaN MQWs at HT-AlN and  $Al_{1-x}Ga_xN/GaN$  SLs based HT-AlN buffer layer.

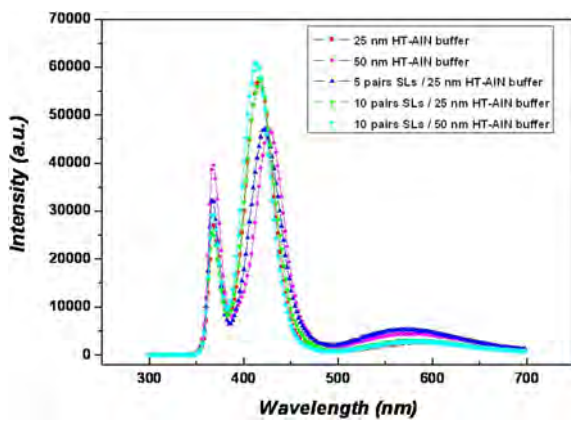


**Fig. 4.** CL spectra of the several GaN pyramids and InGaN/GaN MQWs at HT-AlN and  $Al_{1-x}Ga_xN/GaN$  SLs based HT-AlN buffer layer.

because the patterned dots provide open sites for buffer layer growth on the Si substrates and suppress the random growth of GaN on  $SiO_2$ . The GaN pyramid and InGaN/GaN MQWs had a flat GaN (0002) and six  $\{1\bar{1}01\}$  facets. The pyramidal facets between the top surface of the pyramid structure and  $SiO_2$  were approximately  $60^\circ$ , which suggests the  $\{1\bar{1}01\}$  planes of hexagonal GaN. The difference in growth rate between the (0002) and  $\{1\bar{1}01\}$  planes, which are the rapid growth rate of the (0002) plane and slow growth rate of the  $\{1\bar{1}01\}$  planes, caused the formation of the six well-orientated  $\{1\bar{1}01\}$  facets of the GaN pyramid structures [18].

Fig. 3 shows the room temperature PL spectra from all samples using the 325 nm line from a He-Cd laser as an excitation source. Strong band edge emission peaks of GaN and InGaN/GaN MQWs were observed at approximately 367 nm and 419 ~ 429 nm in all samples. The latter peaks indicated that the InGaN/GaN MQWs were grown homogeneously on the GaN pyramid structures because there were no double peaks and satellite peaks. A comparison of the InGaN/GaN MQWs on HT-AlN (25, 50 nm) buffer layers with inserted  $Al_{1-x}Ga_xN/GaN$  SLs based HT-AlN buffer

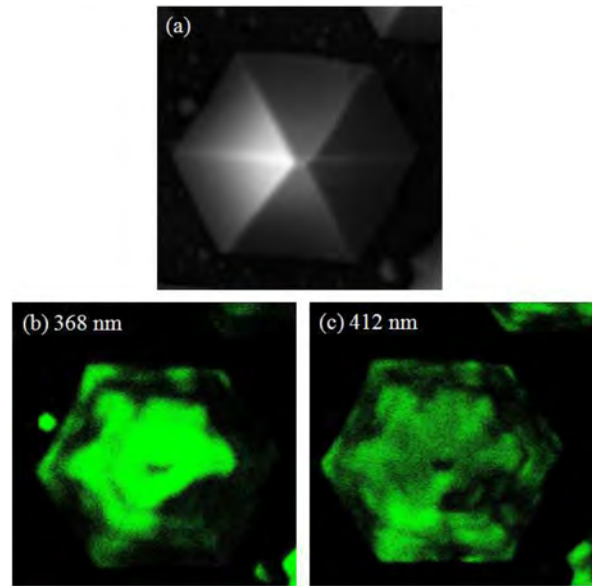


**Fig. 5.** (a) The surface SEM image of the GaN pyramid and InGaN/GaN MQWs on 10 pair of  $Al_{1-x}Ga_xN/GaN$  SLs based 50 nm HT-AlN buffer and monochromatic CL images obtained at (b) 368 nm, (c) 412 nm.

layer showed that the intensity of the emission peaks increased. The increased intensity of the PL spectra was due to a decrease in dislocation density by  $Al_{1-x}Ga_xN/GaN$  SLs. The dislocations act as nonradiative recombination centers at the active region of InGaN/GaN MQWs [19].

To clarify the origin of the emission parts of specific wavelengths on the GaN pyramid and InGaN/GaN MQWs at PL spectra, the CL spectra and monochromatic CL images with an excitation energy 10 keV. Fig. 4 shows the CL spectra, which were obtained from several separated the GaN pyramid and InGaN/GaN MQWs. The CL spectra of the GaN pyramid and InGaN/GaN MQWs were observed at approximately 366 ~ 368 nm and 412 ~ 428 nm. A comparison of the bulk GaN (3.4 eV ~ 365 nm) with the synthesized GaN pyramids at all samples showed a red shift in the emission peaks. In addition, the red shift in InGaN/GaN MQWs emission peaks decreased with increasing pair of  $Al_{1-x}Ga_xN/GaN$  SLs on the AlN buffer layer with various thicknesses. In addition, the red shift in the GaN near band emission and emission peaks of InGaN/GaN MQWs in CL spectra was attributed to the induced tensile stress of GaN on Si. In the case of the InGaN/GaN MQWs, the red shift was affected by compensation tensile stress due to the insertion of different pair of  $Al_{1-x}Ga_xN/GaN$  SLs [20]. The broad emission peak of InGaN/GaN MQWs by CL was attributed to the increased thickness of InGaN/GaN MQWs toward the  $SiO_2$  mask and the difference in indium composition between the top and bottom of the  $\{1\bar{1}01\}$  planes, which were attributed to the difference in growth rates between (0002) and  $\{1\bar{1}01\}$  as well as the diffusion length of Ga and In atoms in the vapor phase [21].

The monochromatic CL surface images (b) and (c) in Fig. 5 were examined at 368 and 412 nm, which were the strong emission peaks of GaN and InGaN/GaN MQWs, respectively. The monochromatic image of InGaN/GaN MQWs at 412 nm corresponds to the radiation and non-radiated region of GaN at the 368 nm monochromatic image. This indicates that the generated and propagated dislocations in the GaN pyramid structures led to a non-radiated sight in the InGaN/GaN MQWs.

### Conclusions

This study examined the effect of an  $\text{Al}_{1-x}\text{Ga}_x\text{N}/\text{GaN}$  SLs based HT-AlN buffer layer on the crystallinity and optical properties of selectively grown GaN pyramids and InGaN/GaN MQWs. The sharpest and narrowest FWHM of the  $\omega$ -scan (0002) rocking curve was  $1.215^\circ$  for the 10-pair  $\text{Al}_{1-x}\text{Ga}_x\text{N}/\text{GaN}$  SLs based 50 nm HT-AlN buffer layer. The strong band edge emission peak of the InGaN/GaN MQWs by the CL measurements was shifted towards a short wavelength with increasing pair of  $\text{Al}_{1-x}\text{Ga}_x\text{N}/\text{GaN}$  SLs due to the induced compressive stress. The emission region of the GaN pyramids and InGaN/GaN MQWs coincide practically. These results suggest that the crystal and optical properties of the selectively grown GaN pyramids and InGaN/GaN MQWs using the SAG technique can be improved by optimizing the relationships between the pair of  $\text{Al}_{1-x}\text{Ga}_x\text{N}/\text{GaN}$  SLs and AlN buffer thickness.

### Acknowledgement

This study was supported by the Samsung Research Fund, Sungkyunkwan University, 2009.

### References

1. F.K. Yam, Z. Hassan, C.K. Tan, C.W. Lim, and A.A. Aziz, *Microelectron. Eng.* 81 (2005) 268-272.
2. S. Vézian, A.L. Louarn, and J. Massies, *J. Cryst. Growth* 303 (2007) 419-426.
3. J. Bai, T. Wang, P.J. Parbrook, I.M. Ross, and A.G. Cullis, *J. Cryst. Growth* 289 (2006) 63-67.
4. J.H. Yang, S.M. Kang, D.V. Dinh, and D.H. Yoon, *Thin Solid Films* 517 (2009) 5057-5060.
5. P. Chen, S.Y. Xie, Z.Z. Chen, Y.G. Zhou, B. Shen, R. Zhang, Y.D. Zheng, J.M. Zhu, M. Wang, X.S. Wu, S.S. Jiang, and D. Feng, *J. Cryst. Growth* 213 (2000) 27-32.
6. S. Raghavan and J.M. Redwing, *J. Appl. Phys.* 98 (2005) 023514.
7. W. Luo, X. Wang, L. Guo, H. Xiao, C. Wang, J. Ran, J. Li, and J. Li, *Microelectron. J.* 39 (2008) 1710-1713.
8. S. Raghavan, X. Weng, E. Dickey, and J.M. Redwing, *Appl. Phys. Lett.* 87 (2005) 142101.
9. B.S. Zhang, M. Wu, J.P. Liu, J. Chen, J.J. Zhu, X.M. Shen, G. Feng, D.G. Zhao, Y.T. Wang, H. Yang, and A.R. Boyd, *J. Cryst. Growth* 270 (2004) 316-321.
10. E. Arslan, M.K. Ozturk, A. Teke, S. Ozcelik, and E. Ozbay, *J. Phys. D-Appl. Phys.* 41 (2008) 155317.
11. S.H. Jang, and C.R. Lee, *J. Cryst. Growth* 253 (2003) 64-70.
12. M.A. Mastro, C.R. Eddy Jr., D.K. Gaskill, N.D. Bassim, J. Casey, A. Rosenberg, R.T. Holm, R.L. Henry, and M.E. Twigg, *J. Cryst. Growth* 287 (2006) 610-614.
13. K. Hiramatsu, K. Nishiyama, A. Motogaito, H. Miyake, Y. Iyechika, and T. Maeda, *Phys. Status Solidi A* 176 (1999) 535-543.
14. Tanaka, Y. Kawaguchi, N. Sawaki, M. Hibino, and K. Hiramatsu, *Appl. Phys. Lett.* 76 (2000) 2701.
15. D.Y. Song, A. Chandolu, N. Stojanovic, S.A. Nikishin, and M. Holtz, *J. Appl. Phys.* 104 (2008) 064309.
16. L.W. Sang, Z.X. Qin, H. Fang, X.R. Zhou, Z.J. Yang, B. Shen, and G.Y. Zhang, *Appl. Phys. Lett.* 92 (2008) 192112.
17. T. Tsuchiya, J. Shimizu, M. Shirai, and M. Aoki, *J. Cryst. Growth* 276 (2005) 439-445.
18. H. Miyake, K. Nakao, and K. Hiramatsu, *Superlattices Microstruct.* 41 (2007) 341-346.
19. K.Y. Zang, Y.D. Wang, H.F. Liu, and S.J. Chua, *Appl. Phys. Lett.* 89 (2006) 171921.
20. Y. Honda, Y. Kuroiwa, M. Yamaguchi, and N. Sawaki, *Appl. Phys. Lett.* 80 (2002) 222.
21. W. Feng, V.V. Kuryatkov, A. Chandolu, D.Y. Song, M. Pandikunta, S.A. Nikishin, and M. Holtz, *J. Appl. Phys.* 104 (2008) 103530.